

Violation of Entropic Leggett-Garg Inequality in Nuclear Spin Ensembles

Hemant Katiyar¹, Abhishek Shukla¹, Rama Koteswara Rao², and T. S. Mahesh^{1*}

¹*Department of Physics and NMR Research Center,*

Indian Institute of Science Education and Research, Pune 411008, India

²*Department of Physics and NMR Research Center, Indian Institute of Science, Bangalore, India*

We report an experimental study of recently formulated entropic Leggett-Garg inequality (LGI) by Usha Devi *et al.* (arXiv: 1208.4491v2 (2012)). This inequality places a bound on the statistical measurement outcomes of dynamical observables describing a macrorealistic system. Such bounds may be violated by quantum systems, and provide an important way to distinguish quantumness from classical behavior. Here we study entropic LGI using an ensemble of spin-1/2 nuclei initialized into a maximally mixed state. We also describe a general method to extract single-event and joint probabilities using an ancilla register. The experimental results show a violation of entropic LGI by over five standard deviations. These results agree with the predictions of quantum theory.

PACS numbers: 03.67.Lx, 03.65.Ta, 03.67.Ac, 76.30.-v

Keywords: Leggett-Garg Inequality, Shannon Entropy, Joint Probabilities

Introduction.— The behavior of quantum systems is often incomprehensible by classical notions, the best examples being nonlocality [1, 2] and contextuality [3]. As a result of nonlocality, quantum systems violate Bell's inequality derived from the assumption that local operations on one of the two space-like separated objects can not disturb the measurement outcomes of the other [4]. The quantum systems are also contextual in the sense that a measurement outcome depends not only on the system and the property being measured, but also on the context of the measurement, i.e., on the set of other compatible properties which are being measured along with.

Another notion imposed on classical objects is macrorealism, which is based on two criteria: (i) the object remains in one or the other of many possible states at all times, and (ii) the measurements are noninvasive, i.e., they reveal the state of the object without disturbing the object or its future dynamics. Quantum systems are incompatible with these criteria and therefore violate bounds on correlations derived from them. For instance, Leggett-Garg inequality (LGI) sets up macrorealistic bounds on linear combinations of two-time correlations of a dichotomic observable belonging to a single dynamical system [6]. LGI may be considered as a temporal analogue of Bell's inequality between two space-like separated systems. Quantum systems do not comply with LGI, and therefore provide an important way to distinguish the quantum behavior from macrorealism. Violation of LGI by quantum systems has been investigated and confirmed experimentally in various systems [7–17].

For understanding the quantum behavior it is important to investigate it through different approaches, particularly from an information theoretical point of view. For example, an entropic formulation for Bell's inequality has been given by Braunstein and Caves [20], and more recently that for contextuality has been given indepen-

dently by Rafael and Fritz [21] and Kurzynski *et al.* [22]. Recently, an entropic formulation of LGI has also been given by Usha Devi *et al.* [18], in terms of classical Shannon entropies associated with classical correlations. Such entropies obey certain constraints, which when violated would imply non-existence of legitimate joint probabilities for all the measurement outcomes.

Here we report an experimental demonstration of violation of entropic LGI in an ensemble of spin 1/2 nuclei using Nuclear Magnetic Resonance (NMR) techniques. Although NMR experiments are carried out at a high temperature limit, the nuclear spins have long coherence times and their unitary evolutions can be controlled in a precise way. As explained in the next section, studying entropic LGI requires the measurement of single-event and joint probabilities. In this article we describe an efficient method to extract these probabilities by exploiting the large parallel computations carried out in an NMR spin ensemble. The method involves simulating a projective measurement in the computation basis by dephasing out the coherences and using an ancilla register to store the single-event and joint probabilities. In the following we briefly revisit theory of the entropic LGI [18].

Theory.— Consider a dynamical observable $Q(t_k) = Q_k$ measured at different time instances t_k . Let the measurement outcomes be q_k with probabilities $P(q_k)$. In classical information theory, the amount of information stored in the random variable Q_k is given by the Shannon entropy [19],

$$H(Q_k) = - \sum_{q_k} P(q_k) \log_2 P(q_k). \quad (1)$$

The conditional information stored in Q_{k+l} at time t_{k+l} , assuming that the observable Q_k has an outcome q_k , is

$$H(Q_{k+l}|Q_k = q_k) = - \sum_{q_{k+l}} P(q_{k+l}|q_k) \log_2 P(q_{k+l}|q_k),$$

where $P(q_{k+l}|q_k)$ is the conditional probability. Then the

mean conditional entropy is given by,

$$H(Q_{k+l}|Q_k) = - \sum_{q_k} P(q_k) H(Q_{k+l}|Q_k = q_k). \quad (2)$$

Using Bayes' theorem, $P(q_{k+l}|q_k)P(q_k) = P(q_{k+l}, q_k)$, the mean conditional entropy becomes

$$H(Q_{k+l}|Q_k) = H(Q_k, Q_{k+l}) - H(Q_k), \quad (3)$$

where the joint Shannon entropy is given by

$$H(Q_k, Q_{k+l}) = - \sum_{q_k, q_{k+l}} P(q_{k+l}, q_k) \log_2 P(q_{k+l}, q_k) \quad (4)$$

These Shannon entropies always follow the inequality [20]

$$H(Q_{k+l}|Q_k) \leq H(Q_{k+l}) \leq H(Q_k, Q_{k+l}). \quad (5)$$

The left side of the equation implies that removing a constraint never decreases the entropy, and right side implies information stored in two variables is always greater than or equal to that in one [18]. Suppose that three measurements Q_k , Q_{k+l} , and Q_{k+m} , are performed at time instants $t_k < t_{k+l} < t_{k+m}$. Then, from equations (3) and (5), the following inequality can be obtained:

$$H(Q_{k+m}|Q_k) \leq H(Q_{k+m}|Q_{k+l}) + H(Q_{k+l}|Q_k). \quad (6)$$

For n measurements Q_1, Q_2, \dots, Q_n , at time instants $t_1 < t_2 < \dots < t_n$, the above inequality can be generalized to [18]

$$\sum_{k=2}^n H(Q_k|Q_{k-1}) - H(Q_n|Q_1) \geq 0. \quad (7)$$

This inequality must be followed by all macro-realistic objects, since its satisfaction means the existence of legitimate joint probability distribution, which can yield all the marginal probabilities [22].

It has been shown that the above inequality is violated by a quantum spin- s system, prepared in a completely mixed initial state, $\rho_{in} = \mathbb{1}/(2s+1)$ [18]. Consider the z -component of the spin evolving under the Hamiltonian $H = \omega S_y$ as our dynamical observable, *i.e.* $Q_t = U_t S_z U_t^\dagger$, where $U_t = e^{-iHt}$, and S_y and S_z are the components of spin-angular momentum. Let n -measurements occur at regular time instants $\Delta t, 2\Delta t, \dots, n\Delta t$. Ideally in this case, the conditional entropies $H(Q_k|Q_{k-1})$ between successive measurements are all equal, and can be denoted as $H[\theta/(n-1)]$, where $\theta/(n-1) = \omega\Delta t$ is the rotation caused by the Hamiltonian in the interval Δt . Similarly we can denote $H(Q_n|Q_1)$ as $H[\theta]$. The lhs of (7) scaled in units of $\log_2(2s+1)$ is termed as the information deficit D . For n -equidistant measurements,

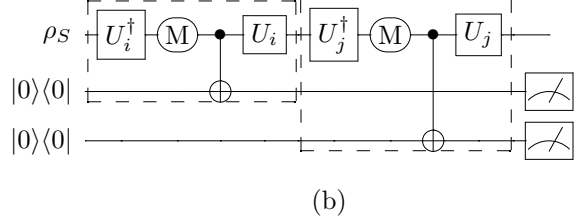
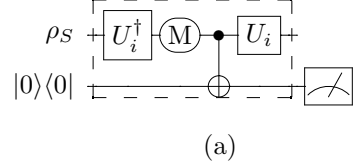


FIG. 1. Circuits for measuring single-event (a) and joint probabilities (b). The grouped gates represent measurement in $\{\Pi_0^t, \Pi_1^t\}$ basis, and M represents measurement in computational basis $\{\Pi_0, \Pi_1\}$. The CNOT gates are used to encode the probabilities on to the ancilla qubits.

it can be written as [18]

$$D_n(\theta) = \frac{(n-1)H[\theta/(n-1)] - H[\theta]}{\log_2(2s+1)} \geq 0. \quad (8)$$

Measurement of Probabilities.— We consider a spin- $1/2$ particle precessing under the Hamiltonian $H = \omega S_y$, and choose its z -component as the dynamical observable. Using the eigenvectors $\{|0\rangle, |1\rangle\}$ of S_z , as the computational basis, the projection operators at time $t = 0$ are $\{\Pi_0 = |0\rangle\langle 0|, \Pi_1 = |1\rangle\langle 1|\}$. For the dynamical observable, the measurement basis is rotating under the unitary $U_t = e^{-i\omega S_y t}$, such that $\Pi_0^t = U_t \Pi_0 U_t^\dagger$ and $\Pi_1^t = U_t \Pi_1 U_t^\dagger$. However, it is usually convenient to carry out all the measurements in the computational basis. Since for an instantaneous state $\rho(t)$, $\Pi_\alpha^t \rho(t) \Pi_\alpha^t = U_t \Pi_\alpha (U_t^\dagger \rho(t) U_t) \Pi_\alpha U_t^\dagger$ (with $\alpha = 0$ or 1), measuring in $\{\Pi_0^t, \Pi_1^t\}$ basis is equivalent to back-evolving the state by U_t , measuring in computational basis, and lastly forward evolving by U_t .

Here we describe a general method to extract the single-event probabilities and joint probabilities of pairs of independent measurements by using ancilla qubits. The method involves the quantum circuits shown in Fig. 1. The system qubit is initially prepared in a general state ρ_S and each ancilla qubit is prepared in the state $|0\rangle\langle 0|$. In Fig. 1a, the state of the system qubit after the evolution U_i^\dagger and subsequent measurement can be written as $P(0_i)|0\rangle\langle 0| + P(1_i)|1\rangle\langle 1|$. The CNOT gate implemented just after the measurement in computational basis encodes the probability of the outcomes in the di-

agonal elements of ancilla qubit since,

$$\begin{aligned} & \{P(0_i)|0\rangle\langle 0|_S + P(1_i)|1\rangle\langle 1|_S\} \otimes |0\rangle\langle 0|_A \\ & \quad \downarrow \text{CNOT} \\ & |0\rangle\langle 0|_S \otimes P(0_i)|0\rangle\langle 0|_A + |1\rangle\langle 1|_S \otimes P(1_i)|1\rangle\langle 1|_A. \end{aligned} \quad (9)$$

The probabilities $P(0_i)$ and $P(1_i)$ can now be retrieved by tracing over the system qubit and reading the diagonal elements of the ancilla state. The final U_i operator which is applied after the CNOT gate does not affect the probabilities stored in the ancilla qubit. The single-event Shannon entropy $H(Q_i)$ is then obtained using eqn. (1). Circuit in Fig. 1b needs to encode outcomes of two measurements, and hence two ancilla qubits are required. Introducing the second ancilla after the first measurement, we obtain ,

$$\begin{aligned} & |0\rangle\langle 0|_S \otimes P(0_i)|00\rangle\langle 00|_A + |1\rangle\langle 1|_S \otimes P(1_i)|10\rangle\langle 10|_A \\ & \quad \downarrow U_j^\dagger U_i, M \\ & \{P(0_i, 0_j)|0\rangle\langle 0| + P(0_i, 1_j)|1\rangle\langle 1|_S\} \otimes |00\rangle\langle 00|_A + \\ & \{P(1_i, 0_j)|0\rangle\langle 0| + P(1_i, 1_j)|1\rangle\langle 1|_S\} \otimes |10\rangle\langle 10|_A \\ & \quad \downarrow \text{CNOT} \\ & |0\rangle\langle 0|_S \otimes P(0_i, 0_j)|00\rangle\langle 00|_A + \\ & |1\rangle\langle 1|_S \otimes P(0_i, 1_j)|01\rangle\langle 01|_A + \\ & |0\rangle\langle 0|_S \otimes P(1_i, 0_j)|10\rangle\langle 10|_A + \\ & |1\rangle\langle 1|_S \otimes P(1_i, 1_j)|11\rangle\langle 11|_A. \end{aligned} \quad (10)$$

In the above, M denotes the measurement in the computational basis, and CNOT is controlled by the system and is acting on the second ancilla as shown in Fig. 1b. The reduced density operator for the ancilla qubits is now

$$\begin{aligned} & P(0_i, 0_j)|00\rangle\langle 00|_A + P(0_i, 1_j)|01\rangle\langle 01|_A + \\ & P(1_i, 0_j)|10\rangle\langle 10|_A + P(1_i, 1_j)|11\rangle\langle 11|_A. \end{aligned} \quad (11)$$

Thus all the joint probabilities are stored as the diagonal elements of the ancilla state. The joint Shannon entropy $H(Q_i, Q_j)$ can then be obtained using eqn. 4. These circuits can be generalized for multiple measurements or for spin- $s > 1/2$ system, using appropriate ancilla register.

In order to study LGI, the system qubit is initially prepared in the maximally mixed state, i.e., $\rho_S = \mathbb{1}/2$, such that all the subsequent measurements are rendered non-invasive. In this case, $P(0_i) = P(1_i) = 1/2$, and the joint probabilities are $P(0_i, 0_j) = |\cos(\theta_{ij}/2)|^2/2 = P(1_i, 1_j)$, and $P(0_i, 1_j) = |\sin(\theta_{ij}/2)|^2/2 = P(1_i, 0_j)$ where $\theta_{ij} = \omega(t_j - t_i)$ [18]. Although the joint probabilities have only two distinct values in theory, the above circuits allow storing each of them separately onto the four diagonal elements of the ancilla state.

For the three-measurement LGI test, one needs to measure the single-event entropies $H(Q_1)$ and $H(Q_2)$, and joint entropies $H(Q_1, Q_2)$, $H(Q_2, Q_3)$, and $H(Q_1, Q_3)$. Since the system qubit initialized in $\mathbb{1}/2$ does not evolve under unitary operators, $H(Q_1) = H(Q_2)$. Further, as

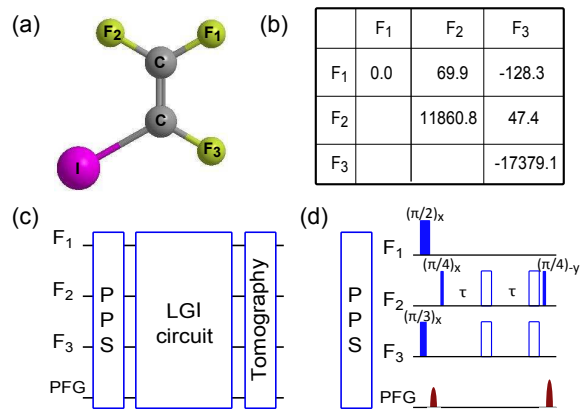


FIG. 2. The molecular structure of trifluoroiodoethylene (a), the table of chemical shifts (diagonal elements) and the J-coupling constants (b), the over-all experimental scheme (c), and the pulse sequence for PPS (d). In (d) the open pulses are π pulses and the delay $\tau = 1/(4J_{12})$.

discussed earlier, if the measurements are carried out at regular intervals, $H(Q_i, Q_{i+1}) = H(Q_{i+1}, Q_{i+2})$. Thus ideally only three entropies: $H(Q_1)$, $H(Q_1, Q_2)$, and $H(Q_1, Q_3)$ are required to be measured to estimate the information deficit D_3 . In the following we describe the experimental implementation of these circuits for the three measurement LGI test.

Experiment.— The qubits are provided by the three spin-1/2 ^{19}F nuclear spins of trifluoroiodoethylene (Fig. 2a) dissolved in acetone- D_6 . The chemical shifts and the scalar coupling constants of the three ^{19}F spins are shown in Fig. 2b. Here F_1 is used as the system qubit and F_2 and F_3 are chosen as the ancilla qubits. Their effective transverse relaxation time constants (T_2^*) were about 800 ms and the longitudinal relaxation time constants were all better than 6.3 s. All the experiments were carried out in a Bruker UltraShield 500 MHz NMR spectrometer at an ambient temperature of 290 K. As illustrated in Fig. 2c, the experiments involved three stages: initialization, implementation of the LGI circuits, and a final diagonal tomography.

Initialization involved preparing the pseudopure state (PPS), $\frac{1-\epsilon}{8}\mathbb{1} + \epsilon\{\frac{1}{2}\mathbb{1}_S \otimes |00\rangle\langle 00|_A\}$ where $\epsilon \sim 10^{-5}$ is the purity factor [23]. The LGI circuits are then carried out as described in Fig. 1. The dynamic propagator is chosen to be S_{1z} precessing under the Hamiltonian ωS_{1y} , with $\omega = 10^3 \text{ rad s}^{-1}$. The propagator $U_t = \exp(-i\omega t S_{1y})$ and the CNOT gates are realized by GRAdient Ascent Pulse Engineering (GRAPE) technique [24]. These consisted of numerically obtained amplitude and phase modulated RF pulses and were robust against the RF inhomogeneity with a average Hilbert-Schmidt fidelity better than 0.998. The measurements in computational basis were realized by using a strong pulsed-field gradient (PFG) which destroyed all the off-diagonal elements of the density matrix

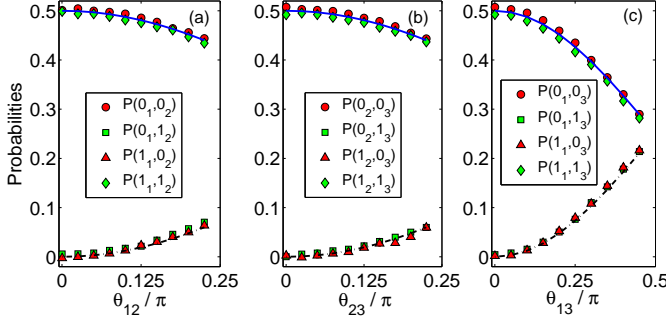


FIG. 3. The symbols indicate the mean experimental probabilities. The solid lines correspond to the theoretical probabilities $P(0_1, 0_2) = P(1_1, 1_2) = c_{12}$ (a), $P(0_2, 0_3) = P(1_2, 1_3) = c_{23}$ (b), and $P(0_1, 0_3) = P(1_1, 1_3) = c_{13}$ (c), with $c_{ij} = |\cos(\theta_{ij}/2)|^2/2$. The dashed lines correspond to the theoretical probabilities $P(0_1, 1_2) = P(1_1, 0_2) = s_{12}$ (a), $P(0_2, 1_3) = P(1_2, 0_3) = s_{23}$ (b), and $P(0_1, 1_3) = P(1_1, 0_3) = s_{13}$ (c), with $s_{ij} = |\sin(\theta_{ij}/2)|^2/2$.

in Zeeman basis.

The diagonal tomography was carried out using a strong PFG to dephase out all the residual off-diagonal elements and using a 5° non-selective linear readout pulse. The resulting intensities of the 12 transitions constrain the 7 independent values (d_i) of the traceless diagonal deviation density matrix. The experimental deviation density matrix is normalized w.r.t. the theoretical traceless density matrix such that they both have the same root mean square value $\sqrt{\sum_i d_i^2}$, and trace is introduced by adding $\mathbb{1}/8$ to the normalized deviation matrix. The probabilities stored in the ancilla part are retrieved by tracing out the system part, and are used to calculate the entropies as described earlier. The experimental and theoretical probabilities used for calculating the joint entropies at various values of evolution angles $\theta = 2\omega\Delta t$ are shown in Fig. 3. Estimation of random errors carried out by several repetitions at each θ value indicate a maximum standard deviation of the probabilities to be 0.008. The deviation between the theoretical and mean experimental probability at each θ value was less than 0.011.

To evaluate the distance between the theoretical (ρ_{th}) and experimental (ρ_{exp}) deviation density matrices, we used fidelity,

$$F = \frac{\text{tr}\{\rho_{\text{th}}\rho_{\text{exp}}\}}{\sqrt{\text{tr}\{\rho_{\text{th}}^2\}\text{tr}\{\rho_{\text{exp}}^2\}}}. \quad (12)$$

The mean fidelity for various values of evolution angles θ are shown in Fig. 4a. Except at the last point ($\theta = 0.45\pi$), the fidelities were above 0.995.

The joint entropies were calculated using the probabilities shown in Fig. 3. Ideally only three entropies are needed to estimate D_3 . The joint entropies $H(Q_1, Q_2)$

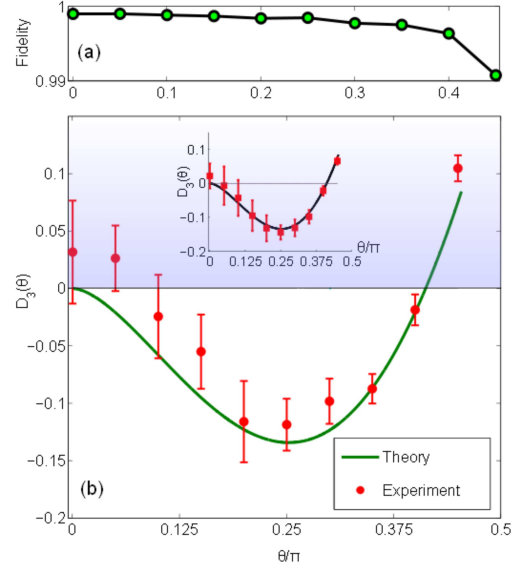


FIG. 4. (a) The mean fidelity plotted versus $\theta = 2\omega\Delta t = \theta_{13}$. (b) Information deficit D_3 versus θ . The curves indicate the theoretical D_3 (in bits). The shaded part indicates the macrorealism territory and the horizontal line at $D_3 = 0$ indicate the macrorealistic lower bound. The mean experimental D_3 (in bits) values are shown in (b) as symbols. The simulated data points shown in the inset of (b) were obtained by adding random errors to the theoretical probabilities as described in the text.

and $H(Q_2, Q_3)$ are separately determined. These allowed us to calculate $H(Q_2|Q_1) = H(Q_1, Q_2) - H(Q_1)$ and $H(Q_3|Q_2) = H(Q_2, Q_3) - H(Q_2)$, although theoretically these two conditional entropies are equal for the equidistant measurements. The information deficit (in bits) was then calculated using the expression $D_3 = H(Q_2|Q_1) + H(Q_3|Q_2) - H(Q_3|Q_1)$. The theoretical and experimental values of D_3 for various rotation angles θ are shown in Fig. 4b. We find a general agreement between the mean experimental D_3 values with that of the quantum theory. The error bars indicate the standard deviations obtained by a series of independent measurements. The lower bound for the macrorealistic systems is indicated by the horizontal line at $D_3 = 0$. The maximum violation by a spin-1/2 particle takes place at $\theta = \pi/4$, which theoretically is $D_3(\pi/4) = -0.134$. Experimentally we found a mean value of -0.119 ± 0.023 . Thus the macrorealistic bound is violated by over five standard deviations.

We observe that small random errors in probabilities cause significant errors in entropy. To illustrate this fact, we have shown in the inset of Fig. 4b, the simulated data points obtained by adding random numbers between -0.005 and $+0.005$ to the theoretical probabilities. It can be seen that the errors in simulated D_3 are significant, particularly for lower values of θ . The errors are less significant for values of θ closer to $\pi/2$. This is due to

the fact that, at lower values of θ , the small probabilities proportional to $\sin^2 \theta$ accumulate higher fractional errors [25]. Systematic errors can also arise due to longitudinal relaxation of the ancilla register.

Conclusions.— We have described a general method to extract single-event and joint probabilities using an ancilla register. Using this method, we demonstrated an experimental study of the entropic Leggett-Garg Inequality on an ensemble of spin-1/2 systems using NMR techniques. Quantum systems do not have legitimate joint probability distribution, which results in violation of bounds set-up for macrorealistic systems. We observed that small random or systematic errors in probabilities leading to significant errors in entropy values. In spite of this, our results indicate the macrorealistic bound being violated by over five standard deviations, confirming the quantum nature of the spin-1/2 particles. One distinct feature of the entropic LGI is that, the dichotomic nature of observables assumed in the original formulation of LGI can be relaxed, thus allowing one to study the quantum behavior of higher dimensional systems such as spin $> 1/2$ systems. This could be an interesting topic for future experimental investigations.

The authors are grateful to Prof. Usha Devi, Prof. Anil Kumar, Dr. Vikram Athalye, and S. S. Roy for discussions. This work was partly supported by the DST project SR/S2/LOP-0017/2009.

* mahesh.ts@iiserpune.ac.in

- [1] A. Einstein, B. Podolsky, and N. Rosen Phys. Rev. **47**, 777 (1935)
- [2] J.S. Bell, Physics **1**, 195 (1964).
- [3] S. Kochen and E. P. Specker, . The problem of hidden variables in quantum mechanics” J. Math. Mech. **17**, 59(1967)
- [4] J. S. Bell, Rev. Mod. Phys. **38**, 447 (1966).
- [5] A. C. Elitzur and L. Vaidman , Found. Phys. **23**, 987 (1993).
- [6] A. J. Leggett and A. Garg, Phys. Rev. Lett. **54**, 857 (1985).
- [7] Xu, J.-S., Li, C.-F., Zou, X.-B. and Guo, G.-C, Sci. Rep. **1**, 101 (2011).
- [8] Yutaro Suzuki, Masataka Inuma, and Holger F. Hofmann, arXiv:1206.6954v2 (2012).
- [9] M. E. Goggina,1, M. P. Almeida, M. Barbieri, B. P. Lanyon, J. L. OBrien, A. G. White, and G. J. Pryde, PNAS **108**, 4 (2011).

- [10] J. Dressel, C. J. Broadbent, J. C. Howell, and A. N. Jordan, Phys. Rev. Lett. **106**, 040402 (2011).
- [11] Vikram Athalye, Soumya Singha Roy, and T. S. Mahesh, Phys. Rev. Lett. **107**, 130402 (2011).
- [12] A. M. Souza, I. S. Oliveira, and R. S. Sarthour, New J. Phy. **13**, 053023 (2011).
- [13] Clive Emary, Phys. Rev. B **86**, 085418 (2012).
- [14] Neill Lambert, Robert Johansson, and Franco Nori, Phys. Rev B **84**, 245421 (2011).
- [15] Knee, G. C. et al., Nat. Commun. 3:606 doi: 10.1038/ncomms1614 (2012).
- [16] Zong-Quan Zhou, Susana F. Huelga, Chuan-Feng Li and Guang-Can Guo, arXiv:1209.2176v1 (2012).
- [17] Yong-Nan Sun, Yang Zou, Rong-Chun Ge, Jian-Shun Tang, Chuan-Feng Li, and Guang-Can Guo, arXiv:1110.5537v2 (2012).
- [18] A. R. Usha Devi, H. S. Karthik, Sudha and A. K. Rajagopal, arXiv: 1208.4491v2 (2012).
- [19] M. A. Nielsen and I. L. Chuang, *Quantum Computation and Quantum Information*, Cambridge University Press (2002).
- [20] S. L. Braunstein and C. M. Caves, Phys. Rev. Lett. **61**, 662 (1988).
- [21] R. Chaves and T. Fritz, Phys. Rev. A **85**, 032113 (2012).
- [22] P. Kurzynski, R. Ramanathan, and D. Kaszlikowski, Phys. Rev. Lett. **109**, 020404 (2012).
- [23] D.G. Cory, M.D. Price and T.F. Havel, Physica D **120**, 82 (1998).
- [24] Navin Khaneja, Timo Reiss, Cindie Kehlet, Thomas Schulte-Herbruggen, and Steffen J. Glaser, J. Magn. Reson. **172**. 296(2005).
- [25] A small error of 0.01 in the measurement of probability can lead to significant error in the entropy, particularly for small probabilities. For example, $0.5 \log_2(0.5) = -0.5000$; $0.51 \log_2(0.51) = -0.495$; $0.001 \log_2(.001) = -0.01$; $0.011 \log_2(0.011) = -0.072$;

Supplementary information.— The equilibrium deviation density matrix evolves under the PPS sequence (Fig. 2d) as follows

$$\begin{aligned}
 & S_{1z} + S_{2z} + S_{3z} \\
 & \quad \downarrow (\pi/2)_{1x}(\pi/3)_{3x}, \text{ PFG} \\
 & S_z^2 + \frac{1}{2}S_{3z} \\
 & \quad \downarrow (\pi/4)_{2x} \\
 & \frac{1}{\sqrt{2}}S_{2z} - \frac{1}{\sqrt{2}}S_{2y} + \frac{1}{2}S_{3z} \\
 & \quad \downarrow 1/(2J_{23}) \\
 & \frac{1}{\sqrt{2}}S_{2z} + \sqrt{2}S_{2x}S_{3z} + \frac{1}{2}S_{3z} \\
 & \quad \downarrow (\pi/4)_{-2y}, \text{ PFG} \\
 & \frac{1}{2}(S_{2z} + 2S_{2z}S_{3z} + S_{3z}).
 \end{aligned}$$